Monofractal and Multifractal Analysis of Discharge Signals in Transformer Pressboards

Serap CEKLI[1], Cengiz Polat UZUNOGLU[2], Mukden UGUR[2]
[1]*Maltepe University, Computer Engineering Department, Istanbul, Turkey*
[2]*Istanbul University, Electrical and Electronics Engineering Department, Istanbul, Turkey*
polat@istanbul.edu.tr

***Abstract*—Pressboards are commonly used as insulating materials employed in electrical connections of transformers. Pressboards are typically made from vegetable fibers, which contain cellulose. The proper operation of power transformer depends mainly on constant monitoring of insulation materials against failure. Due to the complex and close structure of power transformers, it is very challenging task to detect failure and hence possible location of degradation of pressboard internally. Generated discharge signals may result in breakdown of system insulation and system failure. In this study, the investigation of insulation degradation is fulfilled by analyzing discharge signals and simultaneously produced acoustic signals during discharges. For this purpose, a test setup is used for investigating discharge signals of pressboard samples under different electrical stresses. This paper proposes monofractal and multifractal analysis of discharge and acoustic signals of pressboards. The Higuchi's method is an effective monofractal analysis tool for measurement of fractal dimension of self-affine signals, which is proposed for online monitoring of discharge signals of pressboards. In order to investigate obtained discharge signals with accelerated fluctuations effectively, multifractal detrended fluctuation analysis is proposed for these signals, which exhibit nonlinear behavior.**

***Index Terms*—partial discharges, power transformers, fractals, acoustic sensors, power quality.**

I. INTRODUCTION

Power transformers are key elements in electrical power systems, whose insulation construction consist of mineral oil, paper and pressboard (transformer board) [1-3]. The service life of a transformer is strictly related to the insulation performance of the pressboards. Electrical discharges observed on the surface of the pressboard may lead to carbonized tracking patterns and hence accelerate the deterioration and the total breakdown [4-5]. It is a complex task to detect electrical tracking patterns on the pressboard by using real time monitoring systems; hence recent studies have focused on Partial Discharge (PD) characterization and the link between PD and degradation of the pressboard surface [5-9]. In addition to PD analysis, various effects on the mechanical and electrical strength of pressboards have been investigated in literature [10-12]. Moreover, the degradation patterns, which are originated from the surface discharges and penetrated deep inside the pressboards, are analyzed [13-15].

Most of the studies mainly focus on analyzing the relationship between the PD and surface pattern intensity. However, in order to interpret service life and possibility of breakdown, an efficient method for early detection of insulation failure is required. For this purpose, the estimation of pressboard surface distortion by investigating PD signal's characteristics is proposed. The fractal dimension calculation is employed for the analysis of PD signal's characteristics.

Fractal geometry presents a set of mathematical computations for investigating irregular geometric shapes. Fractal geometry and fractal dimension concepts deal with irregular and self-similar images, which are emerged from nature [16-18]. These images, namely fractals have similar subsets in every scale and hence small segments of the fractal figure contain complete figure data without any loss. In the classical geometry objects are computed with integer dimensions, however the fractal geometry estimates non-integer dimensions for fractal figures [19-21].

The monofractal analysis is based on a single parameter (power law exponent) which is fractal dimension of the observed fractal signal [22]. An efficient monofractal computation method for time series analysis of self-affine signals has been introduced by Higuchi in 1988 [23]. In this method, estimation of spectral exponents of complex time series signals are facilitated by employing fractal dimension. The classical fractal dimension calculation processes fractal figure and analyzes figure dynamics. On the other hand, Higuchi's approach for fractal dimension estimation is a very useful method since it assesses time series signals, which are applicable for PDs on the pressboard. Many applications are available to use Higuchi's fractal dimension (HFD), especially in biomedical studies [24-26].

Multifractal signals are analyzed based on power spectrum of power law exponents (dimensions) where fundamental exponent is obviously fractal dimension. Higher order dimensions of this power spectrum is calculated by higher order moments of the fractal dimension [22, 27]. In this study multifractal detrended fluctuation analysis (MDFA) is proposed for multifractal analysis of discharge signals. MDFA method has been recently preferred to reveal multifractal scaling (Hurst exponent) characteristics of complex signals (biomedical studies in general) which have nonstationary statistics [27-30]. MDFA analysis is a robust method to characterize PD signals, which exhibit complex behavior (signal fluctuations) [31].

A test setup is employed for generating surface and sub-surface discharges, which are observed in pressboards. Tests were performed for various AC voltage levels such as 60kV, 70kV and 80kV, which cause different amount of distortion on the surface of pressboard. Although such discharges are generated over time, it is not an easy task to detect these signals with the naked eye, hence monofractal and

Digital Object Identifier 10.4316/AECE.2018.02009

multifractal computation is proposed to observe PD signals on the pressboards. In addition to PD analysis, as an alternative method, a piezo-electric acoustic detector has also been used to obtain and record ultrasonic sounds during PD formation period on the pressboard. These ultrasound signals are analyzed by using monofractal and multifractal methods.

II. Test Setup

Pressboards are prone to exhibit internal and surface damages during their service life as an insulator. To accelerate and simulate these degradations, a test setup has been constructed which enables to generate PDs on pressboard samples in a short time scale. The constructed test setup is given in Fig. 1. For the test procedure all, the pressboards are cut into pieces with dimensions of 300x300x4 mm and for a proper operation; they are initially dried out and soaked with mineral oil in a vacuum medium [32].

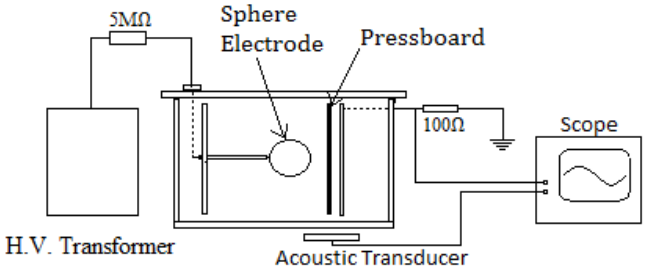

Figure 1. The test setup for pressboard

Pressboard samples are placed in an approximately 5-400mm gap between earthed plane and high-voltage (HV) sphere electrode which is in a chamber full of transformer oil. During the tests all electrical discharges and acoustic signals within the test setup are recorded continuously. The coil of the transformer is simulated with the spherical electrode, which is employed for the modified symmetry of the setup and hence accelerated electrode stresses. A 50kV rated AC voltage is applied to the test cell, which generates a stress similar to typical power system with full-scale 380kV rated transformer. As expected, above these limits (by raising the output voltage of the test transformer up to (percentage160) unexpected discharges and degradations on the pressboards will be initiated. In order to force the system to produce discharges and initiate distortions, the rated voltages of the test transformer have been selected as 60kV, 70kV and 80kV.

The test setup, which is fed by a 100kV single-phase high voltage (HV) transformer and filled with mineral oil, is capable of withstanding up to 100kV. A 5MΩ high voltage resistor is employed for limiting the excessive current during a possible total breakdown. To predict and monitor degradation on the pressboards, a method based on constant monitoring of discharge signals is proposed. For this purpose, the discharge current signal is measured on a 100Ω resistor and recorded by using personal computer. In addition to discharge signal, acoustic noise signals obtained during tests are detected via piezo-electric transducer. Acoustic PD detection has been proposed by many researches [33-35]; all these signals are analyzed and recorded by high-speed oscilloscope.

During tests, surface and subsurface degradation tracking patterns are observed on the pressboards, which usually contain carbonized black spots on the surface. Increased discharges due to increased voltage accelerate surface distortions and finally cause total breakdown and system failure. In this study, an online monitoring system using the HFD estimation method based on discharge signals is proposed. The pressboard samples with surface degradations after a certain test period are given in Fig. 2.

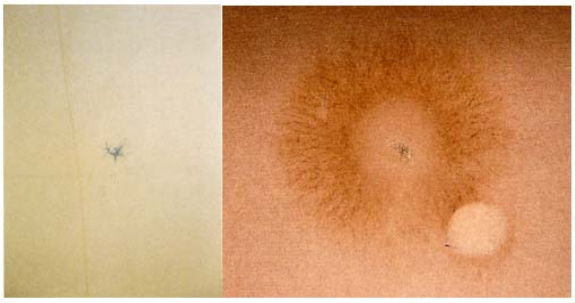

Figure 2. The pressboard samples with surface degradations

III. Higuchi's Fractal Dimension (HFD) Method

Higuchi's algorithm estimates fractal dimension of a time series data directly in the time domain [23]. This method consequently computes fractal dimension by using combinations of various signal lengths *L(k)*. HFD is efficiently computed by the plot (double logarithmic) of *ln(L(k))* versus *ln(k)*. According to relation, which is given in Eq. (1) the exponent D is the fractal dimension of the time series, signal which defines the complexity of the curve [23].

$$L(k) \propto k^{-D} \tag{1}$$

HFD is always calculated between the dimension values of 1 and 2 (it is not required to be integer) since a simple curve has dimension of 1 and a plane has dimension of 2. Selecting proper maximum value of *k* for which the Eq. (1) is approximately linear increases estimation performance [23], [36].

For a discrete time series, such as corresponding sampled PD signal as seen in our scenario can be represented as *X*: *x(1), x(2), x(3),..., x(N)*, with the total data number of *N*. From this time series, new time series X_k^m are obtained (for m=1,2…,k) and given in Eq. (2).

$$X_k^m = \left\{ x(m), x(m+k), x(m+2k), ... \right\} \\ \left\{ ..., x\left(m + \left\lfloor \frac{N-m}{k} \right\rfloor k \right) \right\} \tag{2}$$

In Eq. (2) the ⌊ ⌋ denotes floor function which calculates integer part of a given real number. The k and m are integer numbers, where m represents the initial time and *k* represents interval width respectively. The length of each curve is defined by [26]:

$$L_m(k) = \frac{\alpha}{k} \left[\left(\sum_{i=1}^{\left\lfloor \frac{N-m}{k} \right\rfloor} \left| x(m+ik) - x\left(m+(i-1)k\right) \right| \right) \right] \tag{3}$$

Lm(k) lengths are not the classical lengths but the normalized sums of the absolute values of differences of the values, with a distance denoted by *k* and an initial point *m*. The normalization factor (α) defined for the curve length of time series signal subsets, which is given in Eq. (4).

$$\alpha = \frac{N-1}{\left\lfloor \frac{N-m}{k} \right\rfloor k} \tag{4}$$

In order to calculate length of the curve (*L(k)*) for time interval k, the averaging of all the subseries lengths (Lm(k)) with the corresponding *k* value, is used for *m* = 1, 2, . . . , *k* [23, 36].

$$L(k) = \frac{1}{k}\sum_{m=1}^{k} L_m(k) \tag{5}$$

The HFD is calculated effectively by computing the slope of the linear regression (approximately linear curve required) of a double logarithmic plot of ln *L(k)* versus *ln1/k*. To reduce complexity and to obtain brief expressions the F_1 and F_2 functions are used.

$$F_1 = \ln\left(L(k)\right), \quad F_2 = \ln\left(\frac{1}{k}\right) \tag{6}$$

IV. Multifractal Detrended Fluctuation Analysis

In most cases, it is very challenging task to define complex signal whether it is a monofractal or multifractal signal strictly, since their scaling properties vary due to their axes. It is more appropriate to analyze these signals based on their self-affine characteristics. In the first step, it is required to transform noisy time series data (in our case discharge or ultrasound signals) into time series, which exhibit random walk properties [27].

$$Y(i) = \sum_{k=1}^{i}[x_k - x_{avg}] \qquad i = 1,...,N \tag{7}$$

The average value of the time series signals (x_{avg}) is subtracted from time series signal (x_k) for obtaining random walk like signal. The obtained time series signal contains fluctuations with different magnitudes in small segments of this signal. In order to examine these local fluctuations, the signal is divided into appropriate segments (with equal length s) and related root mean square (RMS) values for these segments are computed [28].

$$Ns \equiv \left\lfloor \frac{N}{s} \right\rfloor \tag{8}$$

Where *Ns* is the number of segments, which is calculated by using the scale s (where non-overlapping segments should be satisfied). In Eq. (8) the floor function is employed. Detrending computation reveals invariant characteristics of these segments (*v*) according to defined scale (which is key element of the self-affine signals). For this purpose, a fitting polynomial $y_v(i)$ is obtained for desired order polynomials. The local trend (fluctuations) can be characterized by using different orders [27]. The variance (second order statistics) is:

$$F^2(s,v) \equiv \frac{1}{s}\sum_{i=1}^{s}\left\{Y\left[(v-1)s+i\right] - y_v(i)\right\}^2, \; v = 1,..N_s \tag{9}$$

By taking the average for all segments, an efficient fluctuation function is derived for desired order (*q*).

$$F_q(s) \equiv \left\{\frac{1}{2N_s}\sum_{v=1}^{2N_s}\left[F^2(s,v)\right]^{q/2}\right\}^{1/q} \tag{10}$$

In Eq. (10) the index variable q can be chosen as any real number. In MDFA method *q* depended fluctuation functions are analyzed. In multifractal signals aside from monofractal signals, various magnitudes of extreme and small local fluctuations are observed. To investigate these characteristics, various order moments are taken into account where q-th order RMS values are computed. The linear regression of this q-th order RMS values result in slopes named Hurst exponent (H_q) for various q values. The q-th order Hurst exponent is one of the key signature of multifractal structure analysis. Using systematic derivations first, the mass exponent (t_q) is derived from q-th order Hurst exponent [27-28].

$$t_q = qH_q - 1 \tag{11}$$

The q-th order singularity exponent (h_q) is derived by using tangent slope of the mass exponent [28].

$$h_q = H_q + qH_q \tag{12}$$

The multifractal dimensions are computed and evaluated for proper analysis. For this purpose, the singularity dimension (D_q) is obtained and expressed by:

$$D_q = \frac{t_q}{q-1}\frac{qh_q - 1}{q-1} \tag{13}$$

Plotting singularity exponent versus singularity dimension provides multifractal spectrum, which is effective tool for investigating multifractal time series. Multifractal spectrum defines arcs of related time series in which multifractal spectrum width is computed by difference of maximum and minimum singularity exponents. Multifractal spectrum width increases with increased multifractal properties. It is noted that multifractal spectrum width is zero for white noise or strictly monofractal time series.

V. Results And Discussion

All the tests are conducted by using selected voltages of 60kV, 70kV and 80kV respectively to simulate over voltages in contrast to power system rated voltages. During the tests, discharge signals and ultrasound signals are recorded via high-speed oscilloscope (N=512 samples). The average values of ten different pressboard samples are processed and analyzed for calculations, which are more accurate. Initially the HFDs of test samples are obtained for each sample and regressive and instantaneous HFD plots are analyzed. PD signals and acoustic signals are processed and corresponding HFDs are calculated separately. In the second part of the study, MDFA is conducted for discharge and ultrasound signals and corresponding figures are obtained.

A. Partial discharge (PD) analysis

During the tests, excessive electrical stresses on the pressboards produced PDs and these PD current signals are collected via a 100Ω resistor. Discharge signals are observed and recorded in extremely short time period (μs). Increased voltage leads to increased PDs on test samples and consequently high intensity surface distortions, which are observed after the test procedures. It is very complex task to intervene a power transformer inner structure and analyze pressboard, while transformer is in operation.

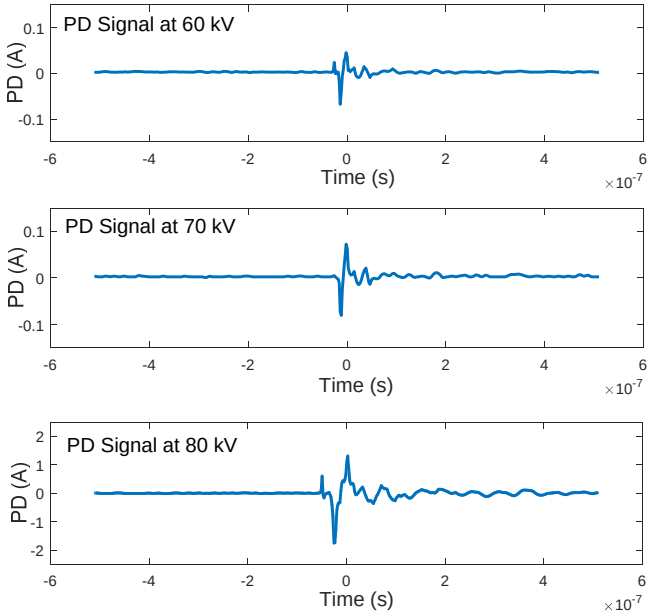

Figure 3. Typical PD current signals on pressboard samples for 60kV, 70kV and 80kV applied voltages

The observed typical PD current signals on pressboard samples for 60kV, 70kV and 80kV applied voltages are given Fig.3. The monofractal HFD method is used for measuring complexity of these PD signals. With the increasing voltage levels, the amplitude of the PD currents are increased as expected. Within a short time period, the number of repeated oscillations decreased with the increased amplitude, which reduces the complexity (frequency of the distortions) of the signal. In our scenario fractal dimension, namely HFD measures the complexity and frequency of the oscillations over time periods. As shown in Fig.4, with the increasing voltage levels the HDFs are decreased respectively. The F_1 and F_2 parameters are ln ($L(k)$) and ln (k) respectively where HFD is calculated by the slope of curve plotted according to these parameters.

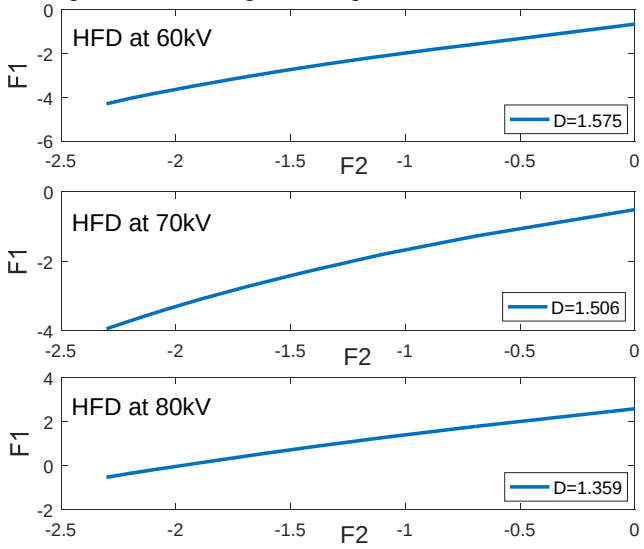

Figure 4. Typical HFD calculation of PD signals on pressboard samples for 60kV, 70kV and 80kV applied voltages

The instantaneous fractal dimensions of PD signals are given in Fig.5 where limited time segments of given time series signal are analyzed and this process is continuously updated for upcoming signal samples instantaneously.

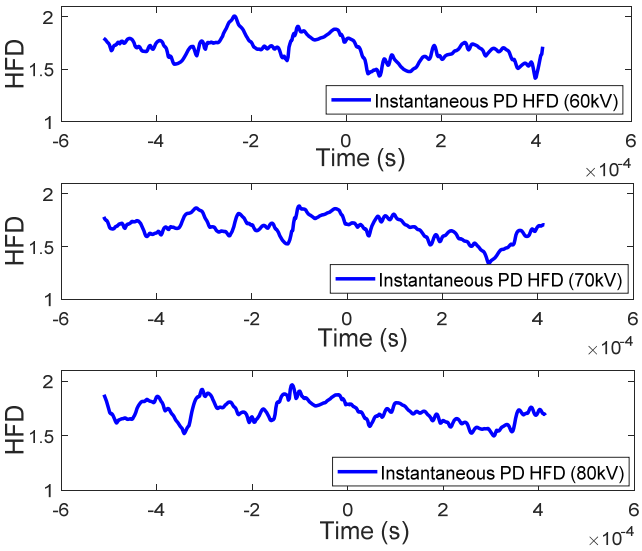

Figure 5. Instantaneous HFD calculation of PD signals on pressboard samples for 60kV, 70kV and 80kV applied voltages

The MDFA is employed for further analysis of recorded discharge signals. The q-order Hurst exponent is derived for discharge signals and given in Fig.6. For negative values of q-orders, Hurst exponent values are quite different for 60kV, 70kV and 80kV applied voltages. The levelling of Hurst exponent lead to truncation of multifractal spectrum.

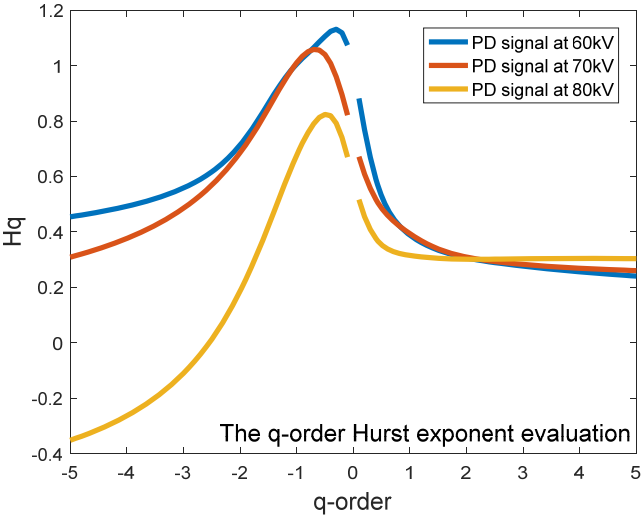

Figure 6. Q-order Hurst exponent evaluation of PD signals on pressboard samples for 60kV, 70kV and 80kV applied voltages

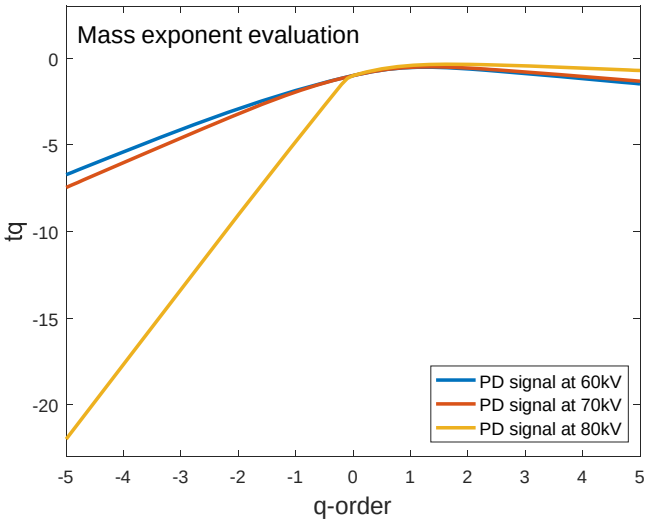

Figure 7. Mass exponent evaluation of PD signals on pressboard samples for 60kV, 70kV and 80kV applied voltages

The mass exponent exhibits multifractal behavior of related time series signals. The mass exponent evaluation of discharge signals is given in Fig.7. Like Hurst exponent, negative values of q-orders the mass exponent values (especially for PD signal at 80kV) are quite different for 60kV, 70kV and 80kV applied voltages. The strict monofractal and white noise time series has linear q dependent mass exponent. Multifractal dimensions (multifractal spectrum) are important parameters for MDFA method. The multifractal spectrum of PD signals is computed and shown in Fig.8. In the spectrum, multifractal signals generate arcs and the width of these arcs define the strength of multifractal behavior. The spectrum width of PD signal at 80kV is quite different from other applied voltages. The long left tail of the corresponding arc is a sign of insensitive multifractal structure to local fluctuations with small magnitude (which is in accordance with our scenario). On the other hand, long right tail means insensitive multifractal structure to local fluctuations with large magnitudes [27].

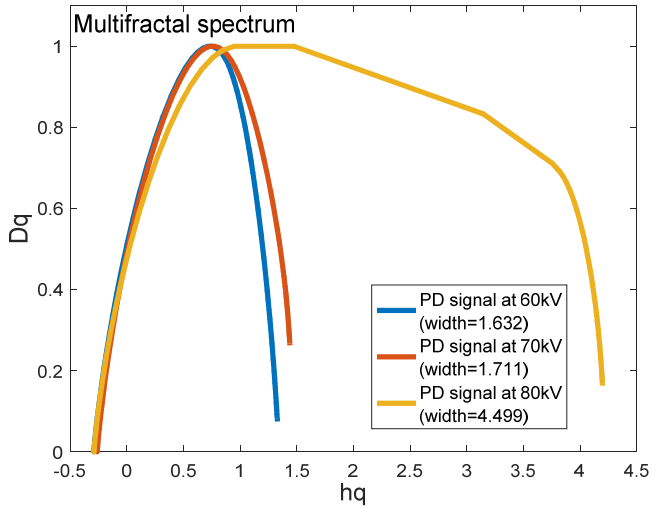

Figure 8. Multifractal spectrum of PD signals on pressboard samples for 60kV, 70kV and 80kV applied voltages

B. *Acoustic noise analysis*

To increase the performance of the proposed method in terms of detecting excessive discharges observed on the pressboards, an additional and distinctive acoustic signal analysis is performed. During the formation of PD signals, ultrasound acoustic signals with higher oscillations are obtained. Repeated oscillations and frequently observed transitions of these signals increase complexity. Typical acoustic noise (ultrasound) signals, which are obtained during tests at 60kV, 70kV and 80kV applied voltages, are given in Fig.9.

Increased applied voltages simultaneously increase amplitudes of the acoustic noise signals. As shown in Fig.9 the amplitude of 80kV test signal is approximately ten times higher than the 60kV test signal. Typical HFD calculations of acoustic noise signals for 60kV, 70kV and 80kV applied voltages are given in Fig.10. During the HFD calculations, linear regressions of F_1 versus F_2 functions are employed. The tests have revealed that the HFD values are slightly decreased with the increasing applied voltages from 60kV to 70kV, however with the 80kV test procedure the complexity of the sound signals and oscillations have decreased significantly, which result in excessive HFD decrease.

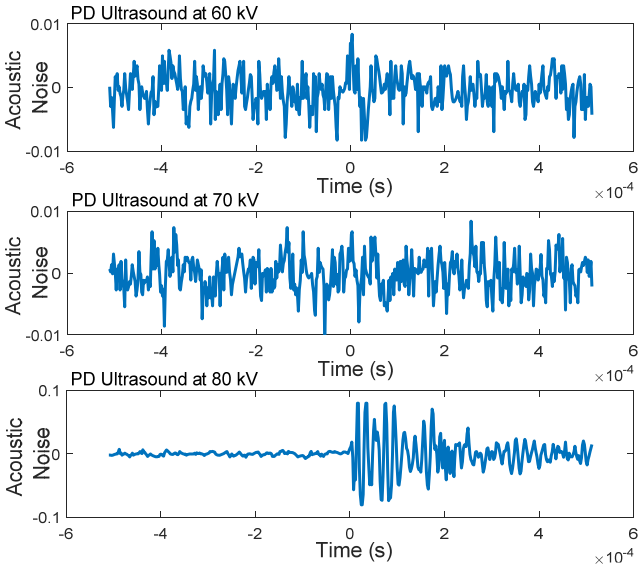

Figure 9. Typical acoustic noise signals obtained from pressboard samples for 60kV, 70kV and 80kV applied voltages

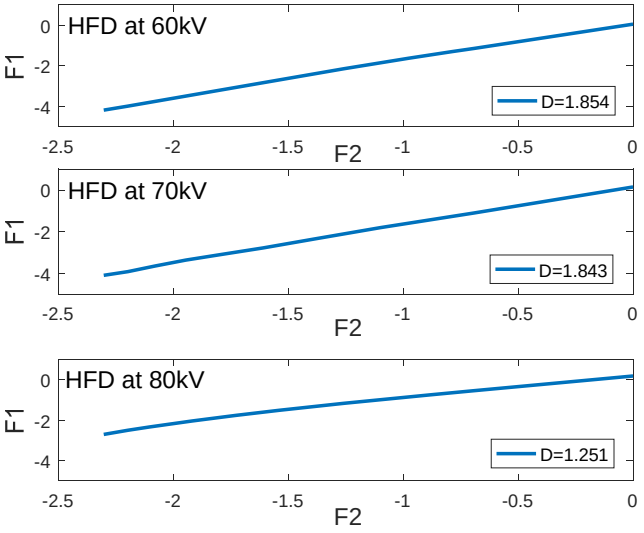

Figure 10. Typical HFD calculation of acoustic noise signals for 60kV, 70kV and 80kV applied voltages

The frequency of oscillations of time signal defines the complexity of the signal. Over voltages cause total breakdown and higher signal amplitudes with less oscillations in a short time period since increased amplitude means reduced peaks in a limited time. As expected the complexity (proportional to the HFD) is reduced with the increased applied voltage.

To obtain proper linear regressions of F_1 versus F_2 functions is much more difficult for increased applied voltages as in 80kV test scenario. A sensitive acoustic sensor used for noise detection, utilizes distortions on pressboards externally since this method processes acoustic noises via piezo-electric transducers. Online processing of these acoustic signals can reveal proper assessment of distortions and hence insulation system failure. As an alternative method aside from classical HFD calculation, the instantaneous HFD of acoustic noise signals are given in Fig.11. This method enables online monitoring of time series signals in terms of fractal dimension. By using instantaneous HFD analysis, the instantaneous complexity of the time series signal especially highly disturbing noise signals with higher frequencies can be investigated.

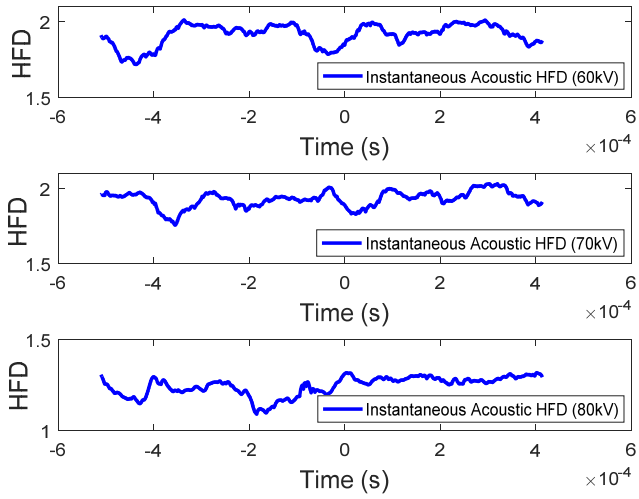

Figure 11. Instantaneous HFD calculation of acoustic noise signals for 60kV, 70kV and 80kV applied voltages

The average HFD calculations for both PD signals and acoustic noise signals are summarized in Table 1. It is clear from Table 1 the average HFD values are decreased with the increasing test voltages. The complexity of acoustic noises is more than PD current signals and hence average HFD values for acoustic signals are higher than average HFD values for PD current signals. Besides acoustic noise, signal HFD calculations are much more distinctive than PD signals in terms of excessive input voltages.

TABLE I. AVERAGE HFD VALUES FOR PD SIGNALS AND ACOUSTIC NOISE SIGNALS

Applied Voltage	Partial discharge signals HFD	Acoustic noise signals HFD
60 kV	1.571	1.852
70 kV	1.501	1.840
80 kV	1.358	1.252

In the second part of the study, MDFA is conducted for acoustic signals. The q-order Hurst exponent evaluation is plotted for acoustic (ultrasound) signals and given in Fig.12.

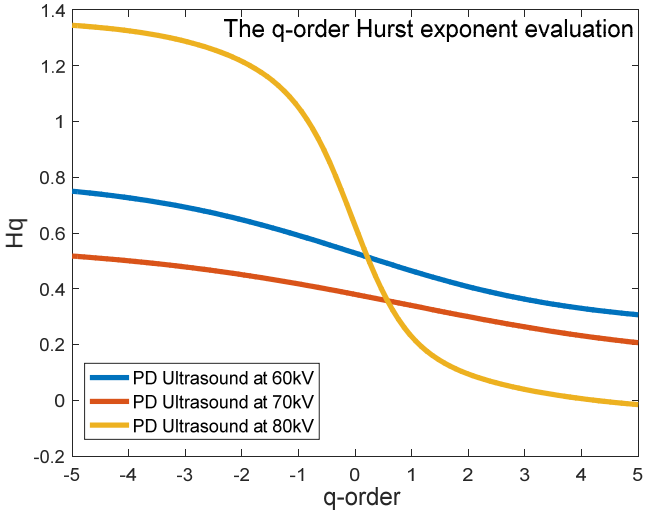

Figure 12. Q-order Hurst exponent evaluation of PD ultrasound signals on pressboard samples for 60kV, 70kV and 80kV applied voltages

Hurst exponent evaluation of acoustic signals for 60kV and 70 kV-applied voltages exhibit stable trends however; Hurst exponent evaluation of acoustic signal for 80kV is quite unstable. For negative q values, the Hurst parameter results are satisfying and distinctive.

The mass exponent evaluation of acoustic signals is given in Fig.13. Mass exponent evaluation of acoustic signals are quite distinctive than the regular PD signals especially for negative q-orders.

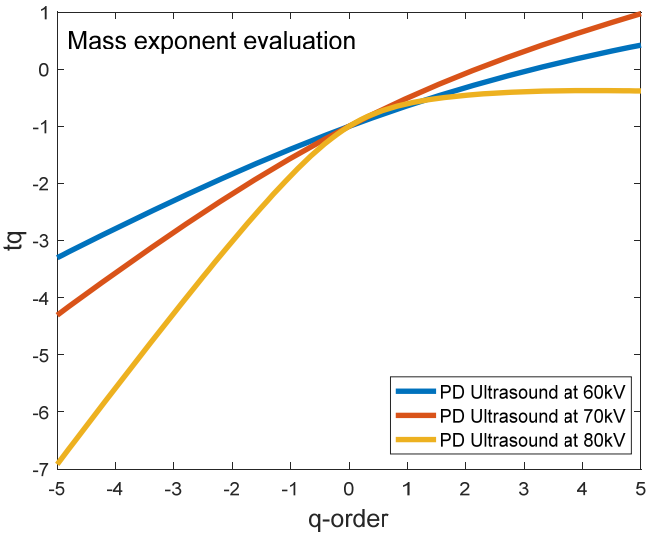

Figure 13. Mass exponent evaluation of PD ultrasound signals on pressboard samples for 60kV, 70kV and 80kV applied voltages

The multifractal spectrum of acoustic signals is given in Fig.14. The spectrum width of acoustic signal at 80kV is quite different from other applied voltages. Increased applied voltage increases the arc widths of the multifractal spectrum. The spectrum of the acoustic signals exhibit relatively long left tails, which means insensitive multifractal structure to local fluctuations with large magnitudes.

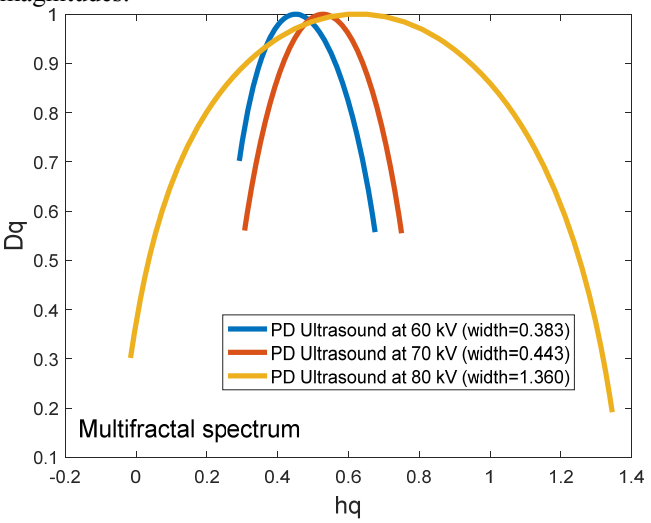

Figure 14. Multifractal spectrum of PD ultrasound signals on pressboard samples for 60kV, 70kV and 80kV applied voltages

VI. CONCLUSION

In this study, the degradative discharge signals observed on pressboard insulations, which are subjected to high electrical stresses, are investigated. In real life operations, excessive voltages generate constant discharges over time and hence distortion patterns on the insulation surface occur consequently. To simulate this phenomenon requires a long period of time naturally, hence a simple test setup was

constructed to conduct discharge tests and to produce artificial breakdown process on pressboard samples. During the tests, to simulate excessive voltages with a proper test setup design, the 60kV, 70kV and 80kV voltages are selected (based on 380kV rated voltage of a typical transmission system) for proposed test procedure. In addition, electrical discharge signals and acoustic noise signals are monitored and recorded. An efficient monofractal HFD algorithm is proposed for discharge detection on pressboards, which can utilize an early warning of insulation failure. The characteristics of these signals can reveal possible breakdown and hence power system failure. Fractal dimension concept can assess complexity of a system especially distortion signals. Tests have uncovered that with the increasing applied over voltages; the system tends produce degradative discharge signals with higher amplitudes. In the early stages of over voltages, the distortions and repeated oscillations are excessive and frequent, however with the increasing over voltages despite the higher amplitudes, the complexity of the signals in terms of oscillations, are decreased. The satisfactory results for both electrical discharge and acoustic noise signals are obtained by using HFD analysis, which showed that the increasing voltage levels causes, decreased HFDs for both acoustic and electrical tests. In order to increase efficiency, MDFA method is conducted for multifractal analysis of discharge signals. The q-order Hurst exponent, mass exponent and multifractal spectrum investigations have revealed the distinctions between the 60kV, 70kV and 80kV applied voltages for both PD and acoustic signals. The proposed HFD and MDFA algorithms are suitable for real time detection and analysis of pressboard failures in which early warning may prevent malfunction of insulation system. Besides, analyzing electrical and acoustic noise signals simultaneously by using combination of these methods improves the performance of the proposed system.

REFERENCES

[1] X. Yi, Z.D. Wang, "Creepage discharge on pressboards in synthetic and natural ester transformer liquids under ac stress," IET Electric Power Applications, vol. 7, no. 3, pp. 191-198, 2013. doi:10.1049/iet-epa.2012.0303

[2] L. Varačka, J. Kúdelčík, M. Gutten, "Dielectric frequency response of mineral oil impregnated pressboard," International Scientific Conference on Electric Power Engineering (EPE), Kouty nad Desnou, 2015, pp. 662-665. doi:10.1109/EPE.2015.7161113

[3] H. P. Mosser, V. Dahinden, Transformerboard II. H.Weidman AG, CH-8640 Rapperswil, pp. 137-144, 1987.

[4] X. Yi, Z.D. Wang, "Surface Tracking on Pressboard in Natural and Synthetic Transformer Liquids under AC Stress," IEEE Trans. Dielectr. Electr. Insul., vol. 20, no. 5, pp. 1625-1634, 2013. doi:10.1109/TDEI.2013.6633692

[5] B. Duan, Y. Cheng, H. Bai, C. Cheng, "A method for on-line monitoring of electric tree growth in pressboard of transformers," IEEE International Conference on High Voltage Engineering and Application (ICHVE), Chengdu, China, pp. 1-4, 2016. doi:10.1109/ICHVE.2016.7800934

[6] C. J. Diao, Y. C. Cheng, et al., "Contrast of the Developing Regularity of Partial Discharge of Oil-paper Insulation Using Step-stress Test and Constant Stress Test," IET High Voltage Engineering, vol. 39, no. 2, pp. 365-373, 2013. doi:10.3969/j.issn.1003-6520.2013.02.017

[7] J. Zhou, J. Li, R. Liao, Y. Lv, "Thermal aging properties of pressboard in mineral oil and natural ester," 2016 IEEE International Conference on High Voltage Engineering and Application (ICHVE), Chengdu, pp. 1-4, 2016. doi: 10.1109/ICHVE.2016.7800759

[8] C. J. Diao, Y. C. Cheng, et al., "Developing Laws and Severity Diagnosis of Partial Discharge Defects on Oil-paper Insulation," IET High Voltage Engineering, vol. 39, no. 5, pp.1061-1068, 2014. doi:10.3969/j.issn.1003-6520.2013.05.006

[9] J. Li, W. Si, X. Yao, Y. Li, "Partial discharge characteristics over differently aged oil/pressboard interfaces," IEEE Transactions on Dielectrics and Electrical Insulation, vol. 16, no. 6, pp. 1640-1647, 2009. doi:10.1109/TDEI.2009.5361584

[10] B. Qi, C. Gao, X. Zhao, C. Li, H. Wu, "Interface charge polarity effect based analysis model for electric field in oil-pressboard insulation under DC voltage," IEEE Transactions on Dielectrics and Electrical Insulation, vol. 23, no. 5, pp. 2704-2711, 2016. doi:10.1109/TDEI.2016.7736829

[11] H. Okubo, T. Sakai, T. Furuyashiki, K. Takabayashi, K. Kato, "HVDC electric field control by pressboard arrangement in oil-pressboard composite electrical insulation systems," IEEE Conference on Electrical Insulation and Dielectric Phenomena (CEIDP), Toronto, pp. 35-39, 2016. doi:10.1109/CEIDP.2016.7785513

[12] F. A. Khan, J. S. Rajan, M. Z. A. Ansari, D. Sivan, "Effects of dibenzyl disulfide on pressboard," IET Chennai 3rd International on Sustainable Energy and Intelligent Systems, Tiruchengode, pp. 1-5, 2012. doi:10.1049/cp.2012.2245

[13] P. M. Mitchinson, P. L. Lewin, B. D. Strawbridge, P. Jarman, "Tracking and Surface Discharge at the Oil–Pressboard Interface," IEEE Electr. Insul. Mag, vol. 26, no. 2, pp. 35-41, 2010. doi:10.1109/MEI.2010.5482553

[14] S. Okabe, G. Ueta, H. Wada, H. Okubo, "PD-induced Degradation Characteristics of Oil-impregnated Insulating Material Used in Oil-immersed Power Transformers," IEEE Transactions on Dielectrics and Electrical Insulation, vol. 17, no. 4, pp. 1225-1238, 2010. doi:10.1109/TDEI.2010.5539694

[15] H. B. H. Sitorus, A. Beroual, R. Setiabudy, S. Bismo, "Creeping discharges over pressboard immersed in jatropha curcas methyl ester and mineral oils," IEEE 11th International Conference on the Properties and Applications of Dielectric Materials (ICPADM), Sydney, pp. 152-155, 2015. doi:10.1109/ICPADM.2015.7295231

[16] B. Mandelbrot, The Fractal Geometry of Nature. Freeman and Co., New York, 1983.

[17] P. A. Burrough, "Fractal dimensions of landscapes and other environmental data," Nature,1 vol. 294, pp.240-242, 1981. doi:10.1038/294240a0

[18] C.P. Uzunoğlu, M. Uğur, A. Kuntman, Simulation of Chaotic Surface Tracking On The Polymeric Insulators With Brownian Motion, Istanbul University – Journal of Electrical & Electronics Engineering, vol.8, no.1, 2008, pp.585-592.

[19] H. G. E. Hentschel, I. Procaccia, "The infinite number of generalized dimensions of fractals and strange attractors," Physica D: Nonlinear Phenomena, vol. 8, no. 3, pp.435-444, 1983. doi:10.1016/0167-2789(83)90235-X

[20] J. Theiler, "Estimating fractal dimension," Journal of the Optical Society of America, vol. 7, no. 6, pp.1055-1073, 1990. doi:10.1364/JOSAA.7.001055

[21] H. Takayasu, Fractals in the Physical Sciences. Manchester University Press, Manchester, 1990.

[22] P. L. Curto-Risso, A. Medina, A. C. Hernández, L. Guzman-Vargas, F. Angulo-Brown, "Monofractal and multifractal analysis of simulated heat release fluctuations in a spark ignition heat engine," Physica A: Statistical Mechanics and its Applications, vol. 389, no .24, pp. 5662-5670, 2010. doi:10.1016/j.physa.2010.08.024

[23] T. Higuchi, "Approach to an irregular time series on the basis of the fractal theory," Physica D: Nonlinear Phenomena, vol. 31, no. 2, pp. 277-283, 1988. doi:10.1016/0167-2789(88)90081-4

[24] C. Gómez, A. Mediavilla, R. Hornero, D. Abásolo, A. Fernández, "Use of the Higuchi's fractal dimension for the analysis of MEG recordings from Alzheimer's disease patients," Med. Eng. Phys, vol. 31, no. 3, pp.306-313, 2009. doi:10.1016/j.medengphy.2008.06.010

[25] S. Kesić, S. Z. Spasić, "Application of Higuchi's fractal dimension from basic to clinical neurophysiology: A review," Computer Methods and Programs in Biomedicine, vol. 133, pp.55-70, 2016. doi:10.1016/j.cmpb.2016.05.014

[26] C. F. Vega, J. Noel, "Parameters analyzed of Higuchi's fractal dimension for EEG brain signals," Signal Processing Symposium (SPSympo), Debe, pp.1-5, 2015. doi:10.1109/SPS.2015.7168285

[27] J. W. Kantelhardt, S. A Zschiegner, E. Koschielny-Bunde, S. Havlin, A. Bunde, H. E. Stanley, "Multifractal detrended fluctuation analysis of nonstationary time series," Phys. A, vol. 316, pp.87–114, 2002. doi: 10.1016/S0378-4371(02)01383-3

[28] N. M. Lau, C. S. Choy, D. H. Chow, "Identifying Multifractality Structure on Postural Sway," Journal of Ergonomics, vol. 15, no. 2, 2015. doi:10.4172/2165-7556.1000137

[29] R. Krishnam, et al., "Detrended fluctuation analysis: a suitable long-term measure of HRV signals in children with sleep disordered

breathing," In: Engineering in Medicine and Biology Society, IEEE-EMBS, pp.1174-1177, 2006. doi:10.1109/IEMBS.2005.1616632

[30] M. Bachmann, A. Suhhova, J. Lass, K. Aadamsoo, U. Võhma, H. Hinrikus, "Detrended fluctuation analysis of EEG in depression," In XIII Mediterranean Conference on Medical and Biological Engineering and Computing, pp.694-697, 2014. doi:10.1007/978-3-319-00846-2_172

[31] S. Kimiagar, et al., "Fractal analysis of discharge current fluctuations," Journal of Statistical Mechanics: Theory and Experiment, vol. 3, pp.3-20, 2009. doi:10.1088/1742-5468/2009/03/P03020

[32] M. El Bari, M. Ruef, M. Renaud, P. Francois, "Drying of Transformer Board," Drying Technology, vol. 14, no. (3-4), pp.825-839, 1996. doi:10.1080/07373939608917126

[33] L. E. Lundgaard "Partial discharge. XIII. Acoustic partial discharge detection-fundamental considerations," IEEE Electrical Insulation Magazine, vol. 8, no. 4, pp.25-31, 1992. doi:10.1109/57.145095

[34] P. J. Moore, I. E. Portugues, I. A. Glover, "Radiometric location of partial discharge sources on energized high-voltage plant," IEEE Transactions on Power Delivery, vol. 20, no. 3, pp.2264-2272, 2005. doi:10.1109/TPWRD.2004.843397

[35] K. Raja T. Floribert, "Comparative investigations on UHF and acoustic PD detection sensitivity in transformers," IEEE International Symposium on Electrical Insulation, Boston, MA, pp.150-153, 2002. doi:10.1109/ELINSL.2002.995900

[36] A. Anier, T. Lipping, S. Melto, S. Hovilehto, "Higuchi fractal dimension and spectral entropy as measures of depth of sedation in intensive care unit," Engineering in Medicine and Biology Society, vol. 1, pp.526-529, 2004. doi.10.1109/IEMBS.2004.1403210